

Video Article

Micropuncture of Bowman's Space in Mice Facilitated by 2 Photon Microscopy

Katsuyuki Matsushita¹, Kirsti Golgotiu¹, Daniel J. Orton², Richard D. Smith², Karin D. Rodland², Paul D. Piehowski², Michael P. Hutchens^{1,3}¹Anesthesiology & Perioperative Medicine, Oregon Health & Science University²Environmental and Biological Services Division, Pacific Northwest National Laboratory³Operative Care Division, Portland Veterans Affairs Medical CenterCorrespondence to: Michael P. Hutchens at hutchenm@ohsu.eduURL: <https://www.jove.com/video/58206>DOI: [doi:10.3791/58206](https://doi.org/10.3791/58206)

Keywords: Biology, Issue 140, Renal physiology, micropuncture, 2-photon microscopy, renal filtrate, Bowman's space, glomerular filtration

Date Published: 10/11/2018

Citation: Matsushita, K., Golgotiu, K., Orton, D.J., Smith, R.D., Rodland, K.D., Piehowski, P.D., Hutchens, M.P. Micropuncture of Bowman's Space in Mice Facilitated by 2 Photon Microscopy. *J. Vis. Exp.* (140), e58206, doi:10.3791/58206 (2018).

Abstract

Renal micropuncture and renal 2-photon imaging are seminal techniques in renal physiology. However, micropuncture is limited by dependence on conventional microscopy to surface nephron features, and 2-photon studies are limited in that interventions can only be assessed at the organ, rather than the nephron level. In particular, micropuncture studies of the glomeruli of mice have been challenged by the paucity of surface glomeruli in mice. To address this limitation in order to pursue studies of aspirate from Bowman's space in mouse physiologic models, we developed 2-photon glomerular micropuncture. We present a novel surgical preparation that allows lateral access to the kidney while preserving the required vertical imaging column for 2-photon microscopy. Administration of high molecular weight fluorescein isothiocyanate (FITC)-dextran is used to render the renal vasculature and therefore glomeruli visible for 2-photon imaging. A quantum dot-coated pipette is then introduced under stereotactic guidance to a glomerulus selected from the several to many which may be visualized within the imaging window. In this protocol, we provide details of the preparation, materials, and methods necessary to carry out the procedure. This technique facilitates previously-impossible physiologic study of the kidney, including recovery of filtrate from Bowman's space and all segments of the nephron within the imaging depth limit, about 100 μm below the renal capsule. Pressure, charge and flow may all be measured using the introduced pipette. Here, we provide representative data from liquid chromatography/mass spectrometry performed on aspirate from Bowman's space. We expect this technique to have wide applicability in renal physiologic investigation.

Video Link

The video component of this article can be found at <https://www.jove.com/video/58206/>

Introduction

The purpose of this procedure is to provide routine micropuncture access to Bowman's space and other glomerular structures in mice. Micropuncture studies for renal physiology have been limited to 1-photon microscopy, which can only image within a few microns of the kidney surface, and which offers limited precision in the z-dimension. Because mice have few surface glomeruli, it is not always possible to find a surface glomerulus by 1-photon microscopy, therefore most micropuncture studies have been carried out in Munich-Wistar rats, which have more numerous surface glomeruli. Therefore, the benefits of working in mouse models have been limited in micropuncture studies^{1,2,3}. Recent advances in imaging technologies, including micro-CT^{4,5}, nanoparticle imaging⁶, and imaging mass spectrometry⁷ have greatly enhanced the range of modalities applicable to glomerular physiology, but there remains no substitute for the unique ability to intervene and sample that micropuncture provides. Therefore extending the use of micropuncture using the techniques presented here is expected to facilitate novel renal physiology studies, in particular, evaluation of the content of renal filtrate (*i.e.*, metabolomics) and basic physiology of transgenic mice, such as measurements of filtrate pressure and charge, previously performed only in rats.

In this technique, use of 2-photon microscopy allows visualization and micropipette access to renal structures up to about 100 μm below the renal capsule. Multiple (5–10) glomeruli are therefore accessible to micropuncture in every mouse kidney thus far imaged. Although this technique shares some features with conventional renal micropuncture, it was designed *de novo* and extensive modifications from conventional technique are required. In this protocol we demonstrate aspiration of fluid from Bowman's space and show example results of subsequent analysis with mass spectrometry (nanoproteomics)^{8,9,10,11}. Downstream use of mass spectrometry requires a specialized sample preparation workflow, which is also demonstrated here.

Protocol

All procedures described herein were approved by the Institutional Animal Care and Use Committee of Oregon Health & Science University.

1. Setup Used for Demonstration

1. Use an upright 2-photon microscope, a 3-axis stage controller, a headstage/pipette holder, and a 3-axis controller for the headstage/pipette holder; all four of these items are required.
NOTE: Many similar setups are available and will suffice as long as independent quantitative 3-axis control of the pipette and microscope stage are available, and the microscope is set up for *in vivo* upright imaging.

2. Materials Necessary Prior to Starting Experimental Protocols

1. Use FITC-dextran, 2,000,000 Da, 5% solution in normal saline or phosphate-buffered saline for retroorbital injection to mark the renal vasculature. This molecular weight (MW) is selected because it remains in the vasculature and does not filter.
2. Machine-pulled borosilicate glass micropipettes: Pull micropipettes to 6–10 μm tip using long-taper, closed tip settings (e.g., heat = 610, velocity = 150, time = 250 ms, looped) on a micropipette puller. Bevel to 45° and flame-polish lightly.
3. Quantum-dot coating of micropipettes: Coat micropipette tips with quantum dots according to the referenced protocol.¹²
4. Polysiloxane kidney support/spacer. Use polysiloxane putty to craft a kidney support/spacer. Fashion a 1 x 1 cm² by 5 mm thick right-angle rhomboid (i.e., a truncated cube) from polysiloxane putty. Remove the middle 70% of the polysiloxane from one edge and a circle comprising about 70% of the center of the rhomboid. Allow the polysiloxane to dry for 24 h. See **Figure 1**.
5. Microinjector preparation: Prefill a length of polyethylene (PE)-50 tubing and the micropipette-loaded micropipette holder with oil. If mass spectrometry is planned, perfluorodecalin is required, otherwise mineral oil may be used. Set up the microinjector with a gas-tight Hamilton-type syringe and fill with perfluorodecalin. This will be connected to the PE-50 tubing and pipette holder.
6. Place the pipette in the pipette holder and forward fill the PE-50 tubing and pipette, then attach the proximal end of the PE-50 tubing to the oil-filled Hamilton syringe, creating a hydraulic system from pipette to syringe.

3. Lateral Pipette Access to The Kidney Below a Fluid Imaging Column via a Novel Surgical Procedure

NOTE: The assembly of the imaging support system and surgical prep is shown in **Figure 1**. The procedure described is performed on C57BL/6 mice weighing 20–25 g.

1. Weigh the mouse.
2. Induce anesthesia using 4% isoflurane and maintain with 1.5–2.5% isoflurane in air/oxygen mixture. Confirm that the mouse is anesthetized by absence of response to painful stimulus and reduced respiratory rate.
3. Lubricate the eyes and position the animal lateral on a baseplate. Immobilize 4 extremities using tape.
4. Inject normal saline, 200 μL , subcutaneously and place a rectal temperature probe. Control temperature using a heating lamp during surgery and a heating pad during imaging.
5. Remove all hair on the left side of the mouse using a depilatory cream.
6. Locate the spleen, which is visible under the skin, and locate the left kidney on the dorsal and caudal side of spleen.
7. Make a 0.5 cm incision on the skin and smaller incision on the peritoneum, just enough for the kidney to push through easily.
8. Extrude the kidney with gentle pressure. Place kidney stabilizer form made with polysiloxane around the kidney and fix with cyanoacrylate adhesive. Line the kidney up with the spacer such that the lateral-most surface of the kidney extends beyond the stabilizer by about 1 mm.
9. Fix a head plate to the stabilizer form with glue and mount the head plate to mounting bars on the base plate.
10. Fill the well in the polysiloxane support surrounding the kidney with 1% agarose solution and place the 10 mm coverslip on top and hold until agarose is firm. Seal coverslip to the head plate with glue and create a ring around the coverslip with dental cement.
11. Inject FITC-dextran (2,000,000 Da, 5% solution, 100–150 μL) retro-orbitally and move the mouse and fixation plate to the 2-photon microscope stage quickly, maintaining anesthesia and ensuring adequate waste gas scavenging on the microscope stage.

4. Selection of a Suitable Glomerulus and Pipette Access to Bowman's Space

1. **Definitions:**
 1. Define X as left-right on the screen and left-right facing the microscope
 2. Read SX (stage X) from the stage controller
 3. Define PX as pipette X, on the pipette dial controller
 4. Define Y as up-down on the screen and forward toward the microscope and back toward the 2-photon setup
 5. Define Z as up toward the ceiling, down toward the floor, and measured on the stage with the objective Z position.
 6. Define S(O)Z as the stage (really the objective) height.
2. **Find the surface of the kidney, identifiable using green fluorescent protein (GFP) filter settings in the ocular. Due to the injection of FITC-Dextran, the vasculature will be bright green.**
 1. Identify a suitable glomerulus. After identifying the surface of the kidney using the ocular, switch to 2-photon (non-scanning mode) and explore the imaging window. Favorable characteristics for micropuncture are the following: vertical distance below the coverslip >30 μm (to prevent collision between the pipette and coverslip during access) and lateral distance from the lateral kidney capsule to the glomerulus <400 μm (beyond this distance the deviation of the pipette may increase likelihood of a miss).
3. Record lateral and vertical distance to the puncture point, a point on the renal capsule directly to the pipette-side of the glomerulus.
4. Raise the objective focal point into the water column, keeping the x and y stage coordinates unchanged, a distance of just about a centimeter.
5. Drive the pipette tip into the water column and turn on 4',6-diamidino-2-phenylindol (DAPI) excitation. Move the pipette in the x and y dimensions to the point of maximal fluorescence of the tip, this will be the center of the objective. Finding the pipette in the ocular is difficult

- without this precise prepositioning. Because quantum dots fluoresce at the same (in this case, red) wavelength regardless of excitation wavelength, the DAPI excitation produces red fluorescence which is tightly focused on the tip, illustrated in **Figure 2**.
6. Change the excitation setting to red fluorescent protein (RFP) and visualize the pipette in the ocular, then precisely center it in the ocular view.
 7. Switch to 2-photon and find the pipette under 2-photon, placing it precisely in the center of the image. This is the registration position.
 8. Save an image of the pipette.
 9. Register the stage and the micropipette controller coordinates.
NOTE: Use the supplemental .html file, which will execute calculations using JavaScript code, (advantageous on systems which do not have installed spreadsheet software) or a spreadsheet to calculate the offset between stage and pipette coordinates and to calculate the target coordinates for the pipette controller.
 10. Remove the pipette from the water column in the x axis, keeping z and y the same.
 11. Move the pipette Z to the target glomerulus Z (*i.e.*, move the pipette down in the Z direction below the coverslip)
 12. Move the pipette Y to the target glomerulus Y coordinate.
 13. Move the 2-photon live view to the target glomerulus Z and then to the edge of the kidney and note the SX.
 14. Calculate the kidney edge PX using the offset from the registration SX.
 15. Move the stage toward the pipette (increase the SX) such that the edge of the kidney is far to the left of the screen, but still visible.
 16. Advance the pipette quickly to about 100 μm less than the kidney edge PX calculated above.
 17. Locate the pipette tip, advancing the pipette slowly. Increase the red gain and watch the red pixel histogram (the pixel distribution shifts before the pipette is imaged in the window, due to the extreme brightness of quantum dots and off-target fluorescence).
 18. Advance to the kidney edge under live 2-photon imaging.
NOTE: Prior to entering the renal capsule, it is possible to redirect the pipette in the Y and Z dimensions. However, this may break the pipette tip. A more conservative measure, if the pipette is off target, is to withdraw in the X dimension up to 2 cm, redirect, and then return in the X dimension to the kidney edge. Once the pipette is within the tissue, movement in any axis other than X leads to pipette flexion which requires great experience to make use of, and frequently leads to breakage.
 19. Drive the pipette in the X axis slowly to the glom target PX, keeping an eye on the SX. (It is helpful to occasionally go back to the glomerulus to see if it has shifted at all upon insertion of the micropipette).
 20. When you are in the correct location, document position with a z-stack.
NOTE: With the micropipette in place, drugs, proteins, or fluorescent tracers may be injected, fluid may be aspirated for later analysis, or pressure or charge relative to another electrode may be measured.

5. Aspiration of Fluid from Bowman's Space

1. Set the micropump to inject 100 nL of perfluorodecalin over 2 min to ensure patency of the pipette and reduce confounding from pipette plugging during entry. Reimage to ensure pipette position.
2. Wait 4–6 min for additional filtration.
3. Set the micropump to aspirate up to 300 nL at a rate of up to 50 nL/min.
NOTE: Changes in glomerular morphology are not observed with this rate, suggesting it does not alter the rate of delivery of fluid to the space during aspiration. As there is no oil block as in conventional micropuncture, recovery of this volume, necessary for mass spectrometry, could include some of the injected perfluorodecalin and possibly tubular fluid. For assays such as ion-sensitive electrode measurements fluorescence spectroscopy, polymerase chain reaction, and other sensitive endpoints, lower volumes may be used. If mass spectrometry is not the endpoint, mineral oil and standard micropuncture techniques can be used to measure the aspirated volume prior to storage.
4. Image once more.
5. Withdraw the pipette and preserve the sample, adding TRIS buffer and storing at -80° prior to analysis.
6. Euthanize the mouse using an overdose of isoflurane or other approved method.
NOTE: Filtrate enters the space by filtration from the glomerular capillaries. The single-nephron glomerular filtration rate (SNGFR) in mice is reported between 8–14 nL/min.³ Starling forces govern SNGFR, however, and negative hydrostatic pressure in Bowman's space therefore may increase SNGFR. Standard micropuncture methods use tubular blockade with oil and neutral pressure for tubular fluid sampling, however these compounds interfere with mass spectrometry (see below); therefore, in this technique the early proximal tubule remains patent. Further, at the time of aspiration, Bowman's space contains an unknown, but positive volume of filtrate. Therefore, fluid aspiration rate may exceed SNGFR.
NOTE: In the experiments described here, the goal was to obtain a larger than usual sample of glomerular filtrate for mass spectrometry analysis by nanoproteomic techniques. Since use of mass spectrometry precludes use of oil blocks with mineral oil or wax (complex mixtures of organic molecules which reduce signal:noise in mass spectrometry) perfluorodecalin is used to fill the micropipette and syringe. Perfluorodecalin is not known to block tubular flow, but is biologically inert and does not interfere with mass spectrometry.

Representative Results

This procedure requires a unique surgical preparation of the kidney for 2-photon imaging and access, which is illustrated in **Figure 1**. This preparation shown here allows a vertical imaging column with the objective above the kidney with few density changes for best-possible optics for 2-photon microscopy simultaneously with lateral access for the pipette, driven exclusively in the horizontal (x) dimension. Partial extrusion of the kidney prevents excess tension on the renal pedicle and preserves vascular flow, and construction of a custom kidney support enables the two objectives of imaging and access. The second challenge in this procedure is precise positioning of the pipette within the kidney in 3 dimensions, which requires registration of the pipette and stage coordinate systems. The critical step for this process is illustrated in **Figure 2**, which shows the pipette being spotted in the water column of the 2-photon microscope under DAPI-excitation. Entering the water column and registering the coordinates of the pipette to those of the stage prior to entering the kidney is critical to enable precise stereotactic positioning of the pipette within the target Bowman's space. The pipette enters the imaging water column from the right. With DAPI excitation turned on, the red quantum dot-coated pipette fluoresces brightly in the red-orange, and it can be carefully positioned under the middle of the objective. As the excitation beam passes through the center of the objective, the pipette may be freely moved to the point of maximum fluorescence, ensuring that it will be visible in the eyepiece.

Proper pipette pulling and glomerulus selection are critical to the success of this protocol, as illustrated in **Figure 3**, **Figure 4**, **Figure 5**. In **Figure 3A**, a properly-pulled, red-fluorescent quantum dot-coated glass micropipette imaged in the fluid column during the pipette registration portion of the procedure can be seen. The tip is 6 microns in width. In **Figure 3B**, a poorly-pulled pipette with 12 μm tip is shown. This pipette cannot penetrate the renal capsule without causing vascular trauma due to the 12 μm diameter and irregular tip surface (note the bur at the top of the bevel). In **Figure 3C** and **3D**, the importance of optimal positioning rather than imaging of the target glomerulus is shown. The beautiful, near-surface glomerulus illustrated in **Figure 3C** demonstrates favorable imaging (due to its surface position at 20 μm below the renal capsule) but would not be suitable for access by this procedure because it is too close to the surface, and the pipette would hit the coverslip. In **Figure 3D**, optimally-positioned glomeruli are shown. Note the different scale used to illustrate both glomeruli (scale bars are all 50 μm). These glomeruli appear less sharp because of refraction caused by depth; this image was taken at 70 μm below the renal capsule. The lateral kidney edge is 250 μm to the right, making both of these glomeruli accessible. During an access procedure, imaging is tightly focused on the target glomerulus as in **Figure 4**, and every-second image acquisition is used, allowing the investigator to precisely observe positioning of the pipette in Bowman's space.

Figure 4 illustrates a typical renal entry and the result, a pipette tip within Bowman's space. In **Figure 4A**, a mean intensity projection from a z-stack with orthogonal views demonstrates the pipette tip in Bowman's space. Note that there is red pipette tip spectral artifact (round ball of fluorescence) due to extremely bright fluorescence of the quantum dots arranged on the conical section of the tip. In **Figure 4B**, a volume projection of z-stack data demonstrates another pipette in Bowman's space. Note that the pipette dragged Bowman's capsule in the direction of travel on entry, creating apparent tenting behind the tip as described in the protocol.

In **Figure 5**, the results of a failed procedure are shown in which a pipette with a too-large opening broke at the renal capsule, causing bleeding. The pipette was too blunt; on attempting to pass the renal capsule, the capsule was pushed ahead of the pipette tip until breakage occurred. In this image, the renal capsule is visible, enhanced by subcapsular bleeding, in FITC-fluorescent green. FITC signal is visible within the pipette itself, indicating that blood under pressure entered the pipette lumen. The arrow points to many red blood cells visible within the pipette lumen as filling defects in the FITC-dextran.

Figure 6 depicts a representative mass spectrum obtained from Bowman's space aspirate, mouse urinary protein 17 (MUP17). Lastly, **Table 1** demonstrates example results of successful aspiration procedures, listing proteins identified using nanoscale mass spectrometry on aspirate collected over 6 minutes from each of 3 mice. In each case, the pipette was imaged as it was withdrawn from Bowman's space, and no FITC fluorescence was observed within Bowman's space or the pipette lumen, indicating lack of aspirate contamination with plasma. 17 proteins, primarily of low molecular weight, were identified from a minimum of 2 unique peptides per protein. Spectral counts are low, consistent with prior estimates of protein in the glomerular filtrate, and known filtered proteins, such as vitamin D binding protein (VTDB), albumin (ALBU), and major urinary protein 17 (MUP17) are present.

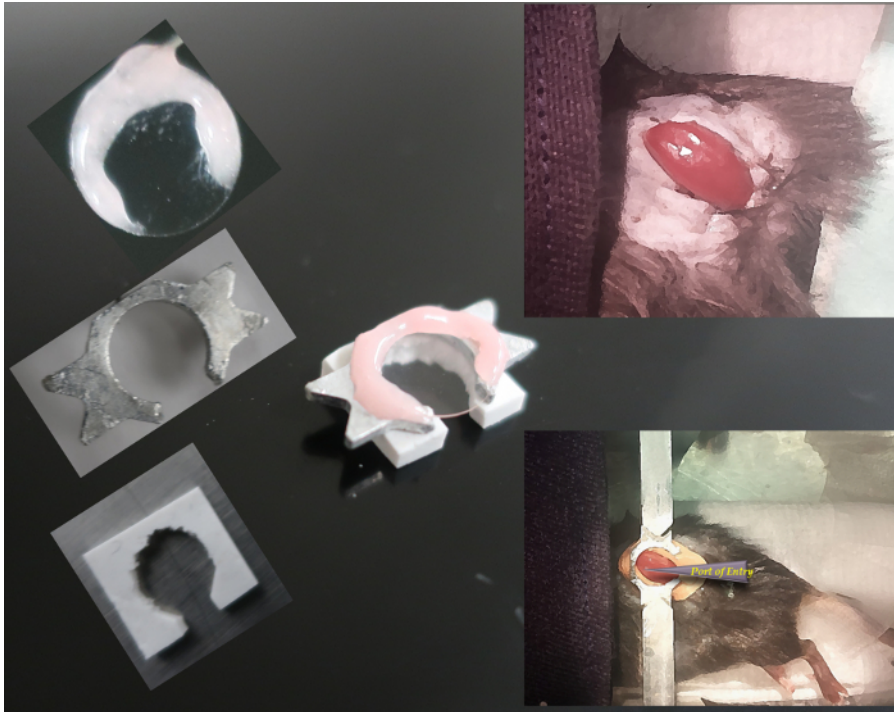


Figure 1: Partial extrusion of the kidney with custom support and immobilization for lateral access. On the left, the parts of the imaging column and kidney support are shown, with the complete assembly in center. On the right, the kidney preparation is shown before (above) and after (below) application of the support. [Please click here to view a larger version of this figure.](#)

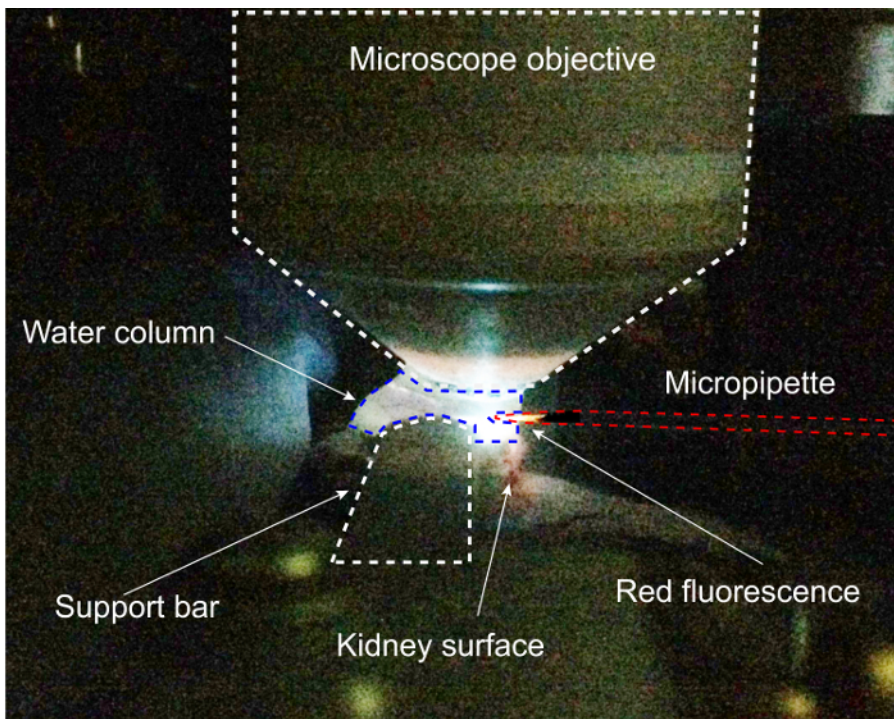


Figure 2: Completed kidney prep at pipette registration step of protocol. Here, DAPI excitation is being used to position the micropipette within the water column of the 2 photon microscope. [Please click here to view a larger version of this figure.](#)

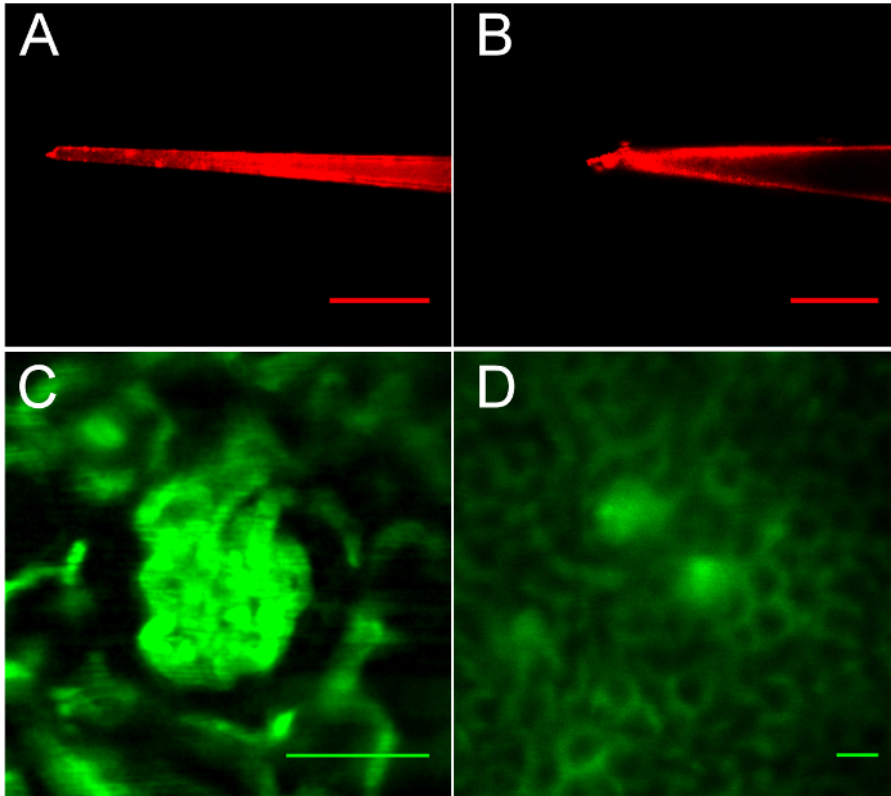


Figure 3: Imaging of pipettes and the kidney after injection of FITC-dextran, demonstrating suitable and unsuitable glomeruli for micropuncture. **A.** A well-pulled pipette with 6 μm tip. **B.** A rough-edged, blunt tip. **C.** This glomerulus is well-defined, but too close to the coverslip for micropuncture. **D.** Suitably positioned glomeruli. Scale bars are all 50 μm . [Please click here to view a larger version of this figure.](#)

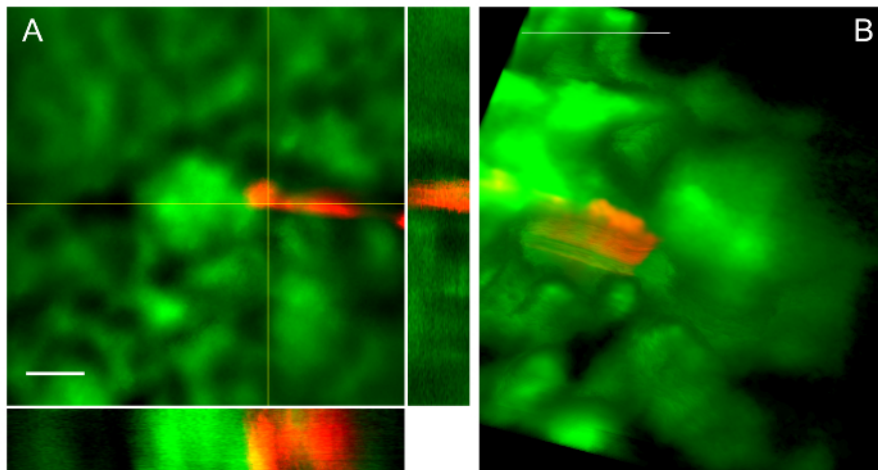


Figure 4: Successful pipette passage leads to placement in Bowman's space-views from 2 different procedures. **A.** Z-stack with orthogonal projections demonstrates pipette tip in Bowman's space abutting the glomerular tuft. Scale bar is 50 μm . **B.** Volume rendering from z-stack similarly demonstrates a pipette in Bowman's space abutting the glomerular tuft. Scale bar is 100 μm . [Please click here to view a larger version of this figure.](#)

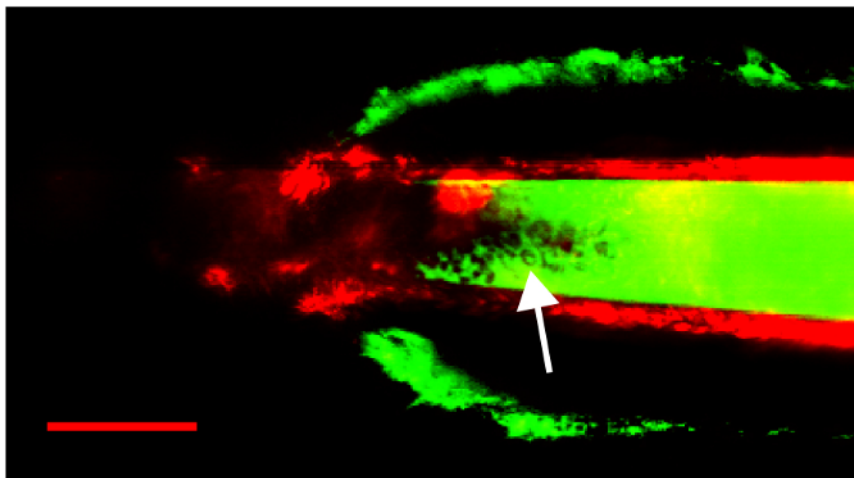


Figure 5: An unsuccessful procedure due to a blunt pipette, tearing the renal capsule and leading to bleeding into the pipette lumen. FITC fluorescence from extravasated plasma, and red blood cells (arrow) are visible within the pipette. Arrow points to red blood cells visible within the pipette lumen. Scale bar is 50 μm . [Please click here to view a larger version of this figure.](#)

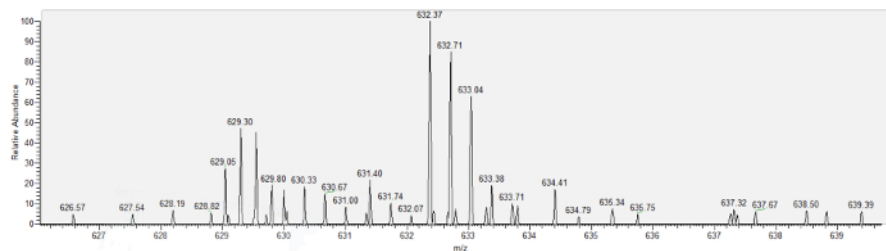


Figure 6: The mass spectrum for major urinary protein 17 (MUP17), obtained from nanoscale liquid chromatography/mass spectrometry analysis of Bowman's space aspirate. [Please click here to view a larger version of this figure.](#)

Protein	MW (kD)	Mean Spectral Count
ACTA_MOUSE	42	2
ACTB_MOUSE	42	1
CLPX_MOUSE	69	2.5
DHSA_MOUSE	73	1
FOLR2_MOUSE	29	1
GBLP_MOUSE	35	1
ALBU_MOUSE	66	6.7
HBA_MOUSE	15	2
HBB1_MOUSE	16	1
MIB1_MOUSE	110	1
MUP17_MOUSE	21	1
PERI_MOUSE	54	1
RNAS4_MOUSE	17	2
SPTB1_MOUSE	2	1
VIME_MOUSE	54	1
VTDB_MOUSE	53	1

Table 1: List of proteins identified in Bowman's space aspirate from 3 mice.

Supplemental Video 1: a volume rendering from a z-stack acquired after positioning a pipette in Bowman's space demonstrates the pipette tip within the space, abutting the capillary tuft. [Please click here to download this file.](#)

Discussion

We present a method to access Bowman's space of non-surface glomeruli in mice, facilitated by 2-photon microscopy. We developed this procedure to address a key limitation of glomerular micropuncture, the rarity of surface glomeruli addressable by 1-photon microscopy in mice, in order to facilitate an experimental objective, aspiration of fluid from Bowman's space for subsequent analysis. Development and practice of this technique rests on six critical steps. First, the novel surgical preparation must be carefully carried out so that the imaging water column does not run off the coverslip and the coverslip extends over the area of kidney which is the target of the pipette. Second, the glass pipette used for micropuncture must be rendered visible for 2-photon microscopy, which is accomplished using quantum dots. Third, stereotactic technique is required to precisely position a pipette in Bowman's space in three dimensions, up to 100 μm below the kidney surface. Therefore, registering the coordinate systems of the pipette and the stage with precision are critical steps. Fourth, careful selection of the target glomerulus is necessary to ensure it is accessible to the pipette without impingement by the kidney support structure and imaging column. Lastly, careful consideration must be given to the analytic steps to follow the acquisition procedure, and volume and timing of acquisition of fluid samples must be matched to the analysis and to glomerular physiology.

We designed an acquisition procedure that may be extended to many analyses, including traditional micropuncture endpoints, such as flame photometry, ion-sensitive electrode measurements, or measurements of pressure, volume or charge. Additionally, we believe this technique will be amenable to novel analytic endpoints including polymerase chain reaction (perhaps following reverse transcription for miRNA) and metabolomics downstream of mass spectrometry. The special modifications employed to facilitate mass spectrometry deserve additional discussion, and they impose some limitations. First, although mass spectrometry is highly sensitive, the low protein content and volume of micropuncture samples renders analysis of protein below the dynamic range of conventional proteomic exploration, and therefore simplified nanoproteomics were necessary.^{8,13} Second, to optimize protein yield for early assays, we determined that 200-300 nL of aspirate was necessary, but *de novo* filtrate acquisition of this volume would require perhaps as long as 20 minutes of aspiration if the mouse GFR is only 8-14 nL/min³. As Tojo and Endou demonstrated that prolonged aspiration alters the albumin content of early proximal tubule fluid¹⁴, we elected to aspirate over 6 minutes; however this means that our aspiration rate exceeds the filtrate inflow rate. Users of this procedure are encouraged to consider the physiology of glomerular filtration in their experimental system in designing their workflow. Mass spectrometry, a sensitive technique, would be overwhelmed by the signal from an introduced petroleum distillate such as mineral oil, which is commonly used in micropuncture to comprise the hydraulic system for aspiration and isolate segments of the nephron. Therefore, we could not use mineral oil for this purpose, or its other common use, quantification of volume of nanoliter range samples. Instead we fill the system with perfluorodecalin which is biologically inert, does not disturb mass spectrometry, and has favorable optical characteristics. We believe the limitations imposed by perfluorodecalin are surmountable and are working on additional technical innovations which we expect will allow measurement of sample volume and blockade of the tubular segment.

Most micropuncture studies have been performed in Munich-Wistar rats, which demonstrate increased numbers of surface glomeruli, but this greatly limited physiologic study of tubular transport and other renal physiology because of the loss of the fundamental tool of molecular biology, transgenic mice^{2,3}. Because it facilitates micropipette access to Bowman's space in mice, the novel technique therefore mitigates these critical limitations. We adopted this technique in order to access renal filtrate for proteomic studies using high-sensitivity mass spectrometry, known as nanoproteomics⁹. However, there are likely additional applications. For example, renal physiologic study of filtered protein has been greatly aided by use of fluorescent tracers with 2-photon microscopy^{15,16,17}. Addition of micropuncture to 2-photon microscopy offers the possibility of performing single-nephron physiologic study with fluorescent molecules, allowing neighboring, non-injected nephrons to serve as controls. It is hoped that this clear explanation of the necessary steps will allow wide adoption in labs already equipped for 2-photon microscopy and/or micropuncture. Although it is complex, we have now performed this procedure many times and the refinements presented herein represent a stable platform for physiologic discovery.

Disclosures

The authors have nothing to disclose.

Acknowledgements

NIDDK K08 DK090754 to **MPH**. **NIGMS** P41 GM103493 to **RDS**. This material is the result of work (by MPH) which was supported with resources and the use of facilities at the Portland Veterans Affairs Medical Center. The contents do not represent the views of the U.S. Department of Veterans Affairs or the United States Government.

References

- Schnermann, J. Micropuncture analysis of tubuloglomerular feedback regulation in transgenic mice. *Journal of the American Society of Nephrology*. **10** (12), 2614-2619 (1999).
- Lorenz, J. N. Micropuncture of the kidney: a primer on techniques. *Comprehensive Physiology*. **2** (1), 621-637 (2012).
- Vallon, V. Micropuncturing the nephron. *Pflügers Archive. European Journal of Physiology*. **458** (1), 189-201 (2009).
- Perrien, D. S. *et al.* Novel methods for microCT-based analyses of vasculature in the renal cortex reveal a loss of perfusable arterioles and glomeruli in eNOS^{-/-} mice. *BMC Nephrology*. **17** 24 (2016).
- Ehling, J. *et al.* Quantitative Micro-Computed Tomography Imaging of Vascular Dysfunction in Progressive Kidney Diseases. *Journal of the American Society of Nephrology*. **27** (2), 520-532 (2016).
- Gimenez, Y. *et al.* 3D Imaging of Nanoparticle Distribution in Biological Tissue by Laser-Induced Breakdown Spectroscopy. *Scientific Reports*. **6** 29936 (2016).

7. Miyamoto, S. *et al.* Mass spectrometry imaging reveals elevated glomerular ATP/AMP in diabetes/obesity and identifies sphingomyelin as a possible mediator. *EBioMedicine*. **7** 121-134 (2016).
8. Piehowski, P. D., Zhao, R., Moore, R. J., Clair, G., & Ansong, C. Quantitative proteomic analysis of mass limited tissue samples for spatially resolved tissue profiling. *Methods in Molecular Biology*. (2017).
9. Yi, L., Piehowski, P. D., Shi, T., Smith, R. D., & Qian, W. J. Advances in microscale separations towards nanoproteomics applications. *Journal of Chromatography A*. **1523** 40-48 (2017).
10. Clair, G. *et al.* Spatially-resolved proteomics: Rapid quantitative analysis of laser capture microdissected alveolar tissue samples. *Scientific Reports*. **6** 39223 (2016).
11. Huang, E. L. *et al.* SNaPP: Simplified nanoproteomics platform for reproducible global proteomic analysis of nanogram protein quantities. *Endocrinology*. **157** (3), 1307-1314 (2016).
12. Andrasfalvy, B. K. *et al.* Quantum dot-based multiphoton fluorescent pipettes for targeted neuronal electrophysiology. *Nature Methods*. **11** (12), 1237-1241 (2014).
13. Huang, E. L. *et al.* SNaPP: Simplified nano-proteomics platform for reproducible global proteomic analysis of nanogram protein quantities. *Endocrinology*. **157** (3), en.2015-1821 (2016).
14. Tojo, A., & Endou, H. Intrarenal handling of proteins in rats using fractional micropuncture technique. *American Journal of Physiology*. **263** (4 Pt 2), F601-606 (1992).
15. Sandoval, R. M., & Molitoris, B. A. Quantifying glomerular permeability of fluorescent macromolecules using 2-photon microscopy in Munich Wistar rats. *Journal of Visualized Experiments*. (74) (2013).
16. Sandoval, R. M., Kennedy, M. D., Low, P. S., & Molitoris, B. A. Uptake and trafficking of fluorescent conjugates of folic acid in intact kidney determined using intravital two-photon microscopy. *American Journal of Physiology: Cell Physiology*. **287** (2), C517-526 (2004).
17. Salmon, A. H. *et al.* Loss of the endothelial glycocalyx links albuminuria and vascular dysfunction. *Journal of the American Society of Nephrology*. **23** (8), 1339-1350 (2012).